Crystallization and preliminary X-Ray diffraction analysis of eukaryotic α_2-macroglobulin family members modified by methylamine, proteases and glycosidases.

Theodoros Goulas[1,*], Irene Garcia-Ferrer[1], Sonia García-Piqué[1], Lars Sottrup-Jensen[2] & F. Xavier Gomis-Rüth[1,*]

[1]Proteolysis Lab, Molecular Biology Institute of Barcelona, CSIC, Barcelona Science Park, Helix Building, c/ Baldiri Reixac, 15-21, E-08028 Barcelona (Spain).

[2]Department of Molecular Biology, Aarhus University, Gustav Wieds Vej 10C, 8000 Aarhus (Denmark).

[*]To whom correspondence should be addressed. Tel: (+34) 934 020 186; Fax: (+34) 934 034 979; E-mail addresses: fxgr@ibmb.csic.es (F.X.Gomis-Rüth) or thgcri@ibmb.csic.es (T. Goulas).

The authors state they have no competing financial interest.

Email addresses

IGF: igfcri@ibmb.csic.es

SGP: soniapique@terra.es

LSJ: lsj@mb.au.dk

ABBREVIATIONS

α_2M: α_2-macroglobulin; hα_2M: human α_2-macroglobulin; MA: methylamine; PNGase F: peptide-N-glycosidase F; Endo F: endo-β-N-acetyl-glucosaminidase F; Tm: melting temperature.

SUMMARY

α_2-Macroglobulin (α_2M) has many functions in vertebrate physiology. In order to understand the basis of such functions, high-resolution structural models of its conformations and complexes with interacting partners are required. In an attempt to grow crystals that diffract to high or medium resolution, we isolated native human α_2M (hα_2M) and its counterpart from chicken egg-white (ovostatin) from natural sources. We developed specific purification protocols, and modified the purified proteins either by deglycosylation or by conversion to their induced forms. Native proteins yielded macroscopically disordered crystals or crystals only diffracting to very low resolution (>20Å), respectively. Optimization of native hα_2M crystals by varying chemical conditions was unsuccessful, while dehydration of native ovostatin crystals improved diffraction only slightly (10Å). Moreover, treatment with several glycosidases hindered crystallization. Both proteins formed spherulites that were unsuitable for X-ray analysis, owing to a reduction of protein stability or an increase in sample heterogeneity. In contrast, transforming the native proteins to their induced forms by reaction either with methylamine or with peptidases (thermolysin and chymotrypsin) rendered well-shaped crystals routinely diffracting below 7Å in a reproducible manner.

INTRODUCTION

The pan-protease inhibitor α_2-macroglobulin (α_2M), together with α_1-macroglobulin, components of the complement cascade (C3, C4 and C5) and pregnancy zone protein, constitute a family of proteins present in all metazoans (Rehman *et al.*, 2013). They contribute to innate immunity and share similar biochemical and structural characteristics, indicating a close evolutionary relationship and a common ancestor (Sottrup-Jensen, 1989; Janssen *et al.*, 2005; Baxter *et al.*, 2007; Fredslund *et al.*, 2008; Marrero *et al.*, 2012). Only recently, proteins of this family have been identified in Gram-negative bacteria, perhaps as a result of more than one horizontal gene transfer event from metazoans (Budd *et al.*, 2004; Doan and Gettins, 2008; Kantyka *et al.*, 2010; Robert-Genthon *et al.*, 2013).

Human α_2M (hα_2M) is a 720-kDa homotetrameric glycoprotein found abundantly in blood plasma. It affords defense against invasive bacteria by trapping their proteases and hampering therefore their successful invasion (Armstrong, 2001). In addition, it regulates endogenous peptidases, and imbalance of its activity leads to several major human diseases (Woessner, 1999; Saunders and Tanzi, 2003; Schaller and Gerber, 2011). Besides its importance as a peptidase inhibitor, α_2M also interacts with several proteins, including defensins, cytokines, growth factors and transferrin, thus participating in diverse and complex regulatory functions (Rehman *et al.*, 2013).

The peptidase inhibitory function of α_2M was recently characterized as a new version of the “Venus flytrap” mechanism (Meyer *et al.*, 2012). Invasive peptidases are confined inside a molecular cage and their action is inhibited by steric hindrance (Marrero *et al.*, 2012). The molecular mechanism starts when a peptidase enters the native inhibitor particle through a narrow opening and cleaves two of the four bait regions of α_2M (Sottrup-Jensen et al. 1989). This induces a large conformational change, which entraps the peptidase within α_2M. At the same time, in a coordinated manner, a second mechanism is induced involving a highly reactive cysteine-glutamine thioester bond, which covalently binds exposed lysines on the attacking peptides, ensuring their entrapment. Induction then exposes a carboxy-terminal domain, the “receptor binding domain”, on the tetramer surface (Sottrup-Jensen 1989). As a result, α_2M is recognized by cell-surface receptors and the complex is internalized by endocytosis and degraded in the lysosomes within minutes of complex formation (Williams *et al.*, 1994). Several α_2Ms have been characterized to date, all sharing the same trapping mechanism. Some, such as ovostatin,

lack an active thioester bond, but they are equally efficient peptidase inhibitors (Rehman *et al.*, 2013).

Structural characterization of α_2M has been extensively addressed since its first isolation by Cohn and co-workers (Cohn *et al.*, 1946). Many attempts to obtain X-ray structural models at high resolution were unsuccessful owing to the poor diffracting properties of the crystals (Andersen *et al.*, 1991; Andersen *et al.*, 1994). Therefore, most research was centred on cryo-electron microscopy models (Stoops *et al.*, 1991; Kolodziej and Schroeter, 1996). Only recently, a 4.3Å resolution model was reported, in which structural details of the methylamine-induced α_2M (α_2M-MA) were described (Marrero *et al.*, 2012). However, in order to understand its mechanism of action and influence in physiology, higher resolution models are required, including that of the native form and models of complexes with peptidases or other interacting molecules. In this context, we examined two α_2M inhibitor homologues: one from human (hα_2M) and the other from chicken egg-white (ovostatin). We assayed several strategies to obtain better diffracting crystals, and thus higher resolution models, in a reproducible manner.

MATERIALS AND METHODS

Isolation and purification of hα_2M and ovostatin. Hα_2M was isolated from blood plasma from individual donors and purified essentially as described (Sottrup-Jensen *et al.*, 1980; Marrero *et al.*, 2012). Briefly, hα_2M in phosphate-buffered saline (pH7.2) was subjected to anion-exchange chromatography in a Q Sepharose column (2.5x10cm) previously equilibrated with 15% buffer A (20mM Hepes, 1M NaCl, pH7.5). A gradient of 20% to 30% buffer A was applied over 150min and fractions were collected in three pools. Selected samples were further fractionated in a TSKgel DEAE-2SW column (TOSOH Bioscience) equilibrated with 2% of buffer B (20mM Tris-HCl,1M NaCl, pH7.5). A gradient of 7% to 20% buffer B was applied over 30ml and samples were collected and pooled. Subsequently, each pool was concentrated and subjected to size-exclusion chromatography in a Superose 6 Prep-Grade column (GE Healthcare Life Sciences) in buffer C (20mM Tris-HCl, 150mM NaCl, pH7.5).

Ovostatin was isolated from egg-white from a single hen and purified as previously described (Nagase *et al.*, 1983). Briefly, after an initial clarification step with 5.5% PEG8000 and removal of aggregates by centrifugation, ovostatin was collected by precipitation with 10% PEG8000 and resuspended in 50mM trisodium citrate, 400mM NaCl, pH6.5. The protein solution was incubated overnight, and precipitated mucins were removed in a Sorvall centrifuge (Thermo Scientific) at 16.000x*g* for 20min at 4^{o}C. Subsequently, the supernatant was passed through a 0.22µm pore size filter (Millipore) and injected into a HiPrep 26/60 Sephacryl S200 column (GE Healthcare Life Sciences). Fractions from the void volume were collected and further purified by anion-exchange chromatography in a 6ml Resource Q column (GE Healthcare Life Sciences) with a gradient from 14% to 24% of buffer B in 10 column volumes. Selected samples were purified with a TSKgel DEAE-2SW column using a linear gradient from 2% to 25% of buffer B within 40 column volumes. The protein was finally polished with a Superose 6 Prep-Grade in buffer C.

Proteins were routinely concentrated with Vivaspin 2 centrifugal filter devices (Sartorius Stedim Biotech) with a molecular-mass cut-off of 30 or 50kDa. All purification steps were performed at 4^{o}C.

Expression and purification of glycosidases. All expression trials were performed in lysogeny broth supplemented with 100μg/ml ampicillin. Glutathione-S-transferase fusions of peptide-N-glycosidase F (PNGase F) and endo-β-N-acetyl-glucosaminidase F1 (Endo F1) (kindly provided by Yoav Peleg, Israel) were expressed in *E. coli* M15 cells overnight at 20^{o}C or for 5h at 37^{o}C, respectively (Grueninger-Leitch *et al.*, 1996). Proteins were purified by affinity chromatography with a GST-Hitrap column (GE Healthcare Life Sciences). Endo F2 and Endo F3 (kindly provided by Patrick Van Roey, USA) fused to maltose-binding protein were expressed as inclusion bodies in *E. coli* BL21 (DE3) cells for 6h at 37^{o}C and subsequently isolated, refolded and purified by anion-exchange chromatography as previously described (Reddy *et al.*, 1998; Waddling *et al.*, 2000). Cells were routinely broken with a cell disrupter (Constant Cell Disruption Systems) at a pressure of 1.35Kbar for soluble proteins and 1.9Kbar for inclusion bodies. Purified proteins were stored at -20^{o}C after a buffer exchange with a PD10 column (GE Healthcare Life Sciences) to 50mM Tris-HCl pH8.0, 25% glycerol for PNGase F or 50mM trisodium citrate pH5.5, 25% glycerol for Endo F1, F2 and F3. Activity of glycosidases was verified with the glycoprotein ribonuclease B (New England Biolabs) at a weight ratio of 1:5 (enzyme:substrate) and a final substrate protein concentration of 0.5mg/ml. Reactions were incubated overnight at 4^{o}C and analysed by SDS-PAGE. Acetyl-neuraminyl hydrolase (sialidase) from *Clostridium perfringens* was purchased from New England BioLabs.

Induction and deglycosylation of hα_2M and ovostatin. Native hα_2M was converted to the induced form by treatment with 200mM methylamine hydrochloride (MA) for 30min at room temperature in 100mM Tris-HCl, 150mM NaCl, pH8.0. Reactions of hα_2M or ovostatin with different ratios of *Bacillus thermoproteolyticus* thermolysin or chymotrypsin from bovine pancreas (both from Sigma-Aldrich) were performed for 1h at room temperature in buffer D (50mM Tris-HCl, 150mM NaCl, pH7.5), except for reactions with thermolysin, in which 5mM $CaCl_2$ was also included. Reactions were stopped with 4mM 4-(2-aminoethyl) benzenesulfonyl fluoride (Pefabloc SC, FLUKA) for chymotrypsin or 5mM 1,10-phenanthroline for thermolysin.

Desialylation trials were performed at an hα_2M or ovostatin protein inhibitor concentration of 1mg/ml in 50μl reaction volumes with 20mM Hepes, 25mM NaCl, pH7.5

as buffer. Different sialidase units (from 1 to 50) were tested and the reactions were incubated overnight at 37°C. Deglycosylation of the proteins was performed overnight at 4°C in weight ratios ranging from 1:10 to 1:500 of glycosidase:inhibitor. Reactions with PNGase F and Endo Fs were performed, respectively, in 50mM Tris-HCl, 50mM NaCl, pH7.5 and 50mM Hepes, 50mM NaCl, pH6.5. Subsequently, glycosidases were trapped by affinity chromatography in a GST-Trap or MBP-Trap column, and deglycosylated α_2M samples were collected from the flow-through. Modified inhibitors were further purified by anion-exchange chromatography and size exclusion chromatography as described above.

Thermal shift assays. Aliquots were prepared by mixing 7.5µl of 300x Sypro Orange dye (Molecular Probes), 5µl protein solution (2.5-5mg/ml in buffer B), and 37.5µl of buffer B. The samples were analyzed in an iCycler iQ Real Time PCR Detection System (BioRad) by using 96-well PCR plates sealed with optical tape. Samples were heated from 20°C to 90°C at a rate of 1°C/min and the change in absorbance (λ_{ex}=490nm; λ_{em}=575nm) was monitored over time. The melting temperature (T_m) was determined for the native and deglycosylated forms of the inhibitors.

Proteolytic activity assays. Proteolytic activity with thermolysin or chymotrypsin trapped in α_2M complexes was routinely measured with the fluorescence-based EnzCheck assay kit containing BODIPY FL-casein (10µg/ml) as a fluorescent conjugate (Invitrogen) at λ_{ex}=485nm and λ_{em}=528nm by using a microplate fluorimeter (FLx800, Biotek). Reactions were performed in buffer D at room temperature (Goulas *et al.*, 2011).

Crystallization, crystal optimization and data analysis. Initial crystallization assays were performed by the sitting-drop vapor diffusion method with protein concentrations ranging from 4mg/ml to 20mg/ml. Reservoir solutions were prepared by a Tecan robot and 100nl crystallization drops were dispensed on 96×2-well MRC plates (Innovadyne) by a Cartesian (Genomic Solutions) nanodrop robot at the IBMB/IRB High-Throughput Crystallography Platform (PAC) of the Barcelona Science Park. Plates were stored in a crystal-farm (Nexus Biosystems) at constant temperatures (4°C and 20°C). Successful crystallization hits were scaled up to the microliter range with 24-well Cryschem or VDX

crystallization dishes (Hampton Research) in sitting or hanging drop format, respectively. Conditions were optimized by varying the initial crystallization conditions and protein concentration, by performing crystal seeding and by including different additives (Hampton Research). Controlled crystal dehydration was performed with the Free Mounting System (FMS; Proteros Biostructures) in an adjustable and reproducible stream of humidified gas, with relative humidity ranging from 70%-98% in 2% increments. A cryocooling protocol was established consisting of either successive passages through reservoir solution containing increasing concentrations of glycerol (up to 20%) or direct immersion of crystals mounted on a loop in Fomblin Y oil. Thereafter, crystals were flash-vitrified in liquid nitrogen and stored. Crystals were checked for X-Ray diffraction at beam lines ID23-1 and ID23-2 of the European Synchrotron Radiation Facility (ESRF, Grenoble, France) at 100K, which were provided with an ADSC Q315R CCD detector and a Mar/Rayonix 3x3 Mosaic 225 detector, respectively. Access to the synchrotron was assigned within the block allocation group "BAG Barcelona." Collected datasets were processed with the XDS/XSCALE package (Kabsch, 2010).

Miscellaneous. Denatured protein samples were analyzed by 10%-15% Tricine-SDS-PAGE (Schägger, 2006) and native proteins by 5% Tris-glycine native PAGE (Haider *et al.*, 2011) and stained with Coomassie-brilliant blue.

Protein concentrations were routinely determined by absorbance at λ=280nm, and wherever necessary corrected by the BCA protein assay method (Thermo Scientific) using bovine serum albumin as a standard. Protein identification by peptide mass fingerprinting was performed at the Protein Chemistry Facility of Centro de Investigaciones Biológicas in Madrid (Spain).

RESULTS

Deglycosylation of hα$_2$M and ovostatin. The inhibitors were isolated from individual human donors (hα$_2$M) or from eggs from a single chicken (ovostatin), and the proteins were purified by a range of chromatographic techniques, applying strict fractionation to maximize sample homogeneity and purity (Fig. 1A). At this point, both inhibitors were subjected to deglycosylation with several glycosidases of variable substrate specificity: sialidase, PNGase F and three Endo Fs (F1, F2 and F3). In particular, treatment of ovostatin with increasing amounts of sialidase had no detectable effect as evaluated by native PAGE (Fig. 1B). In contrast, hα$_2$M was efficiently desialylated in overnight reactions with one sialidase unit per 50ng of protein, showing a reduction in its electrophoretic mobility (Fig. 1C). Digestion with PNGase F or Endo Fs induced a variety of changes in both proteins, thus indicating (at least partial) removal of attached glycosides. In the case of hα$_2$M, the effect of PNGase F was detectable only in native PAGE, and was especially strong at high glycosidase:inhibitor ratios (1:10; see Fig. 1D). On the other hand, Endo Fs at ratios ranging from 1:100 to 1:500 efficiently deglycosylated hα$_2$M, as shown by SDS-PAGE (Fig. 1F). Moreover, digestion with Endo F2 and F3 gave more homogeneous samples than with Endo F1. In ovostatin, deglycosylation was observed in similar level with all the enzymes except Endo F3, which induced minor changes (Fig. 1G). As with hα$_2$M, a larger amount of PNGase F was required to achieve detectable modification in comparison to Endo Fs. Deglycosylation of both proteins was even stronger when all the enzymes were used in combination, thus substantiating a synergistic effect. Deglycosylation was also assessed by a comparative thermal shift assay, in which the temperature of midtransition (Tm) of native and deglycosylated native forms were recorded (Fig. 1H). The Tm of the latter species was systematically lower than that of the former, thus indicating a reduction in thermal stability by ablation of sugars.

Induction of hα$_2$M and ovostatin. Native inhibitors were converted to their activated forms by treatment with peptidases. In addition, hα$_2$M was also activated with methylamine but ovostatin, which lacks a thioester bond, was not. Deglycosylated hα$_2$M showed the characteristic change in electrophoretic mobility in native PAGE after activation by breaking the thioester bond with methylamine, indicating that deglycosylation had no

significant effect on the behavior of the protein (Fig. 1E) (Barrett *et al.*, 1979). Also, the inhibitory function of the protein was unaffected, as observed after reaction with thermolysin at various concentrations (Fig. 1I). Proteolysis resulted in the formation of a pair of bands that ran as 75- and 95-KDa species in SDS-PAGE, as reported elsewhere (Sottrup-Jensen *et al.*, 1981). At molar ratios of protease:inhibitor higher than 2:1, complete digestion of hα_2M was observed, accompanied by a sudden increase in the proteolytic activity due to inhibition release. Similarly glycosylated ovostatin was also activated with either chymotrypsin or thermolysin, which split the protein into the two characteristic bands, accompanied by an increase in the remaining activity at ratios higher than 2:1 (Fig. 1J).

Crystallization and X-ray diffraction. Crystallization trials of native Hα_2M yielded small irregular crystals (Fig. 2A and Table 1). Optimization by varying chemical reagents or crystal seeding was unsuccessful. Moreover, after deglycosylating the protein, only spherulites unsuitable for X-ray diffraction studies were obtained under various conditions (Fig. 2B). Subsequently, conversion of the proteins to their induced forms, by either methylamination or reaction with thermolysin, resulted in several distinct well-shaped crystals (Fig. 2C, D, E and F). Several hundreds of these were collected and tested for diffraction: they routinely yielded diffraction up to 7-8Å (Table 1). Exceptionally, one crystal coming from glycosylated and methylamine-activated protein yielded a complete dataset to 5.9Å resolution (Table 2 and Fig. 3A). This was isomorphous to the single crystal obtained previously, which was used to solve the structure to 4.3Å resolution (Marrero *et al.*, 2012).

Native ovostatin, in turn, yielded nicely shaped crystals which, however, only diffracted to >20Å (Fig 2G). Accordingly, several optimization trials were performed by varying the crystallization conditions, screening several additives and modifying the protein by deglycosylation, but with no success. However, after a systematic trial to dehydrate the crystals by overnight incubation in increasing concentrations of glycerol, an overall improvement of the diffraction to 10Å was observed. Further, based on this observation, a controlled dehydration experiment with the Free Mounting System was performed, during which crystals were treated in relative humidity conditions between 70% and 98%. Unfortunately, this strategy was also unsuccessful. The complex of induced ovostatin with thermolysin, in turn, yielded only thin, fragile needles that did not diffract (Fig 2H). In contrast, ovostatin induced with chymotrypsin gave well-shaped crystals (Fig. 2I), which

diffracted to better than 7Å (Fig. 3B). One complete dataset was collected and processed to 6.7Å, revealing an orthorhombic space group and four molecules per asymmetric unit (Table 2).

DISCUSSION

Due to their significance in vertebrate physiology, the peptidase inhibitors of the α_2M family of proteins have been subjected to extensive research for almost seventy years. One of the aims is to obtain medium- or high-resolution structural models to explain their mechanism of function, which was achieved only recently with methylamine-treated glycosylated hα_2M (Marrero *et al.*, 2012). Over the last few decades, besides the technological advances in protein crystallography through the routine availability of synchrotron radiation and sensitive CCD and pixel detectors, several efforts have focused on improving crystal quality and achieving reproducible results, but without major breakthroughs. The weak crystal diffraction can be attributed mainly to sample heterogeneity owing to glycosylation and the intrinsic flexibility of target proteins (Andersen *et al.*, 1991; Andersen *et al.*, 1994).

In an attempt to increase the resolution of our current hα_2M model, we examined two orthologs—one from human and the other from chicken— which were isolated from fluids of different function and had low sequence similarity (<44.5%). Both proteins were isolated and purified from individual sources to maximize sample homogeneity, an important step to ensure a protein sample as homogenous as possible and to avoid heterogeneity associated with raw material of various origins. However, this did not provide suitable crystals for hα_2M or ovostatin. A significant reproducible improvement in diffraction was observed after dehydration of ovostatin crystals. This indicated that the crystals had a large water content and loose packing, which are common problems associated with low resolution and poor-quality diffraction, as reported for several protein crystals in the past (Andersen *et al.*, 1991; Heras and Martin, 2005). In parallel, local disorder in crystal packing, perhaps due to slightly different conformations of segments of the eleven subunits of individual α_2M tetramers, may also explain their regularly-shaped or low diffracting crystals. α_2M has two different forms, depending on whether it is induced by proteases. The induced form adopts a more close conformation that is more robust and has lower solvent content (Barrett *et al.*, 1979; Marrero *et al.*, 2012). In accordance with

these observations, activation of the glycosylated proteins with either methylamine or peptidases reproducibly yielded crystals diffracting to better than 7Å.

Hα$_2$M and ovostatin are glycoproteins with a high carbohydrate content (Dunn and Spiro, 1967; Nielsen *et al.*, 1994; Paiva *et al.*, 2010). Glycosylation is an important posttranslational modification in eukaryotic proteins, and it plays role in proper protein folding and stability but also in protein function (Walsh *et al.*, 2005; Chang *et al.*, 2007). In contrast to the positive effect on protein folding and function, glycosylation is, in general, highly deleterious for crystallogenesis, since it hinders the necessary crystal contacts or introduces microheterogeneity into the protein sample (Baker *et al.*, 1994; Grueninger-Leitch *et al.*, 1996). Therefore, hα$_2$M and ovostatin were treated with various glycosidases, all of which removed glycosides to a certain extent. The best results were obtained after combined use of PNGase F and the three Endo Fs assayed. Sialidase was effective on hα$_2$M but not on ovostatin. However, as removal of glycosides with these enzymes simultaneously entailed removal of the sialic acid moieties at the terminating branches of N-glycans (Varki and Schauer, 2009), sialidase alone was not used for subsequent experiments with hα$_2$M. Crystallization trials with deglycosylated forms of both native hα$_2$M and ovostatin only resulted in spherulites in the best cases. This indicated that deglycosylation either increased heterogeneity or exacerbated protein stability, factors which are highly correlated with crystallization probability (Ericsson *et al.*, 2006).

Overall, the crystallization trials presented here indicate that modification of the α$_2$M-like protein inhibitors by glycosidases is not a favorable approach. Only conversion of the protein to the activated form rendered more reproducible results, although still at low resolution. Therefore, more crystallization conditions and methods need to be tested in order to obtain suitable samples for high resolution diffraction studies.

ACKNOWLEDGEMENTS

We are indebted to Tibisay Guevara for her outstanding dedication during crystallization experiments and assistance throughout the life of the project, and to Robin Rycroft for substantial contributions to the manuscript. We are also grateful to the IBMB/IRB Crystallography Platform (PAC) in Barcelona. This study was supported in part by grants from European, Spanish, and Catalan agencies (FP7-HEALTH-2010-261460 "Gums&Joints"; FP7-PEOPLE-2011-ITN-290246 "RAPID"; FP7-HEALTH-2012-306029-2"TRIGGER"; BFU2012-32862; CSD2006-00015; Fundació "La Marató de TV3" grant 2009-100732; and 2009SGR1036). We acknowledge the help provided by ESRF synchrotron local contacts. Funding for travelling and synchrotron data collection was provided in part by ESRF.

LITERATURE

Andersen, G.R., Jacobsen, L., Thirup, S., Nyborg, J., and Sottrup-Jensen, L. (1991) Crystallization and preliminary X-ray analysis of methylamine-treated alpha-2-macroglobulin and 3 alpha-2-macroglobulin-proteinase complexes. *FEBS* **292**: 267–270.

Andersen, G.R., Koch, T., Sorensen, A., *et al.* (1994) Crystallization of proteins of the alpha-2-macroglobulin superfamily. *Ann New York Acad Sci* **10**: 444–446.

Armstrong, P.B. (2001) The contribution of proteinase inhibitors to immune defense. *Trends Immunol* **22**: 47–52.

Baker, H., Day, C., Norris, G., and Baker, E. (1994) Enzymatic deglycosylation as a tool for crystallization of mammalian binding proteins. *Acta Crystallogr D* **50**: 380–384.

Barrett, A.J., Brown, M.A., and Sayers, C.A. (1979) The electrophoretically "slow" and "fast" forms of the alpha-2-macroglobulin molecule. *Biochem J* **181**: 401–418.

Baxter, R.H.G., Chang, C., Chelliah, Y., Levashina, E.A., and Deisenhofer, J. (2007) Structural basis for conserved complement factor-like function in the antimalarial protein TEP1. *Proc Natl Acad Sci* **104**: 11615–11620.

Budd, A., Blandin, S., Levashina, E.A., and Gibson, T.J. (2004) Bacterial alpha-2-macroglobulins: Colonization factors acquired by horizontal gene transfer from the metazoan genome? *Genome Biol* **5**: R38.1–R38.13.

Chang, V.T., Crispin, M., Aricescu, A R., *et al.* (2007) Glycoprotein structural genomics: Solving the glycosylation problem. *Structure* **15**: 267–73.

Cohn, E.J., Strong, L.E., Hughes, W.L., *et al.* (1946) Preparation and properties of serum and plasma proteins. IV. A system for the separation into fractions of the protein and lipoprotein components of biological tissues and fluids. *J Am Chem Soc* **68**: 459–475.

Doan, N., and Gettins, P.G.W. (2008) alpha-Macroglobulins are present in some Gram-negative bacteria: Characterization of the alpha-2-macroglobulin from Escherichia coli. *J Biol Chem* **283**: 28747–28756.

Dunn, J., and Spiro, G.R. (1967) The alpha-2-macroglobulin of human plasma. *J Biol Chem* **242**: 5556–5563.

Ericsson, U.B., Hallberg, B.M., DeTitta, G.T., Dekker, N., and Nordlund, P. (2006) Thermofluor-based high-throughput stability optimization of proteins for structural studies. *Anal Biochem* **357**: 289–298.

Fredslund, F., Laursen, N.S., Roversi, P., *et al.* (2008) Structure and influence of a tick complement inhibitor on human complement component 5. *Nat Immunol* **9**: 753–760.

Goulas, T., Arolas, J.L., and Gomis-Rüth, F.X. (2011) Structure, function and latency regulation of a bacterial enterotoxin potentially derived from a mammalian adamalysin/ADAM xenolog. *Proc Natl Acad Sci* **108**: 1856–1861.

Grueninger-Leitch, F., D'Arcy, A., D'Arcy, B., and Chène, C. (1996) Deglycosylation of proteins for crystallization using recombinant fusion protein glycosidases. *Protein Sci* **5**: 2617–2622.

Haider, S.R., Sharp, B.L., and Reid, H.J. (2011) A comparison of Tris-glycine and Tris-tricine buffers for the electrophoretic separation of major serum proteins. *J Sep Sci* **34**: 2463–2467.

Heras, B., and Martin, J.L. (2005) Post-crystallization treatments for improving diffraction quality of protein crystals. *Acta Crystallogr D Biol Crystallogr* **61**: 1173–1180.

Janssen, B.J.C., Huizinga, E.G., Raaijmakers, H.C. A, *et al.* (2005) Structures of complement component C3 provide insights into the function and evolution of immunity. *Nature* **437**: 505–511.

Kabsch, W. (2010) XDS. *Acta Crystallogr D Biol Crystallogr* **66**: 125–32.

Kantyka, T., Rawlings, N.D., and Potempa, J. (2010) Prokaryote-derived protein inhibitors of peptidases: A sketchy occurrence and mostly unknown function. *Biochimie* **92**: 1644–1656.

Kolodziej, S., and Schroeter, J. (1996) The novel three-dimensional structure of native human alpha-2-macroglobulin and comparisons with the structure of the methylamine derivative. *J Struct Biol* **116**: 366–376.

476 Marrero, A., Duquerro, S., Trapani, S., *et al.* (2012) The crystal structure of human alpha-
477 2-macroglobulin reveals a unique molecular cage. *Angew Chem Int Ed Engl* **51**: 3340–
478 3344.

479 Meyer, C., Hinrichs, W., and Hahn, U. (2012) Human alpha-2-macroglobulin-another
480 variation on the venus flytrap. *Angew Chem Int Ed Engl* **51**: 5045–5047.

481 Nagase, H., Harris, E.D., Woessner, J.F., and Brew, K. (1983) Ovostatin: A novel
482 proteinase inhibitor from chicken egg white. I. Purification, physicochemical properties and
483 tissue distribution of ovostatin. *J Biol Chem* **258**: 7481–7489.

484 Nielsen, K., Sottrup-Jensen, L., Nagase, H., Thorgensen, H., and Etzerodt, M. (1994)
485 Amino acid sequence of hen ovomacroglobulin (ovostatin) deduced from cloned cDNA.
486 *DNA Seq* **5**: 111–119.

487 Paiva, M.M., Soeiro, M.N.C., Barbosa, H.S., Meirelles, M.N.L., Delain, E., and Araújo-
488 Jorge, T.C. (2010) Glycosylation patterns of human alpha-2-macroglobulin: Analysis of
489 lectin binding by electron microscopy. *Micron* **41**: 666–673.

490 Reddy, A., Grimwood, B.G., Plummer, T.H., and Tarentino, A.L. (1998) High-level
491 expression of the Endo-beta-N-acetylglucosaminidase F2 gene in E. coli: One step
492 purification to homogeneity. *Glycobiology* **8**: 633–636.

493 Rehman, A.A., Ahsan, H., and Khan, F. (2013) alpha-2-Macroglobulin: A physiological
494 guardian. *J Cell Physiol* **228**: 1665–1675.

495 Robert-Genthon, M., Casabona, M.G., Neves, D., *et al.* (2013) Unique features of a
496 Pseudomonas aeruginosa alpha-2-macroglobulin homolog. *MBio* **4**: e00309–13.

497 Saunders, A.J., and Tanzi, R.E. (2003) Welcome to the complex disease world. alpha-2-
498 Macroglobulin and Alzheimer's disease. *Exp Neurol* **184**: 50–53.

499 Schägger, H. (2006) Tricine-SDS-PAGE. *Nat Protoc* **1**: 16–22.

500 Schaller, J., and Gerber, S.S. (2011) The plasmin-antiplasmin system: Structural and
501 functional aspects. *Cell Mol Life Sci* **68**: 785–801.

502 Sottrup-Jensen, L. (1989) alpha-Macroglobulins: Structure, shape, and mechanism of
503 proteinase complex formation. *J Biol Chem* **264**: 11539–11542.

504 Sottrup-Jensen, L., Petersen, T.E., and Magnusson, S. (1980) A thiol-ester in alpha-2-
505 macroglobulin cleaved during proteinase complex formation. *FEBS Lett* **121**: 275–279.

506 Sottrup-Jensen, L., Petersen, T.E., and Magnusson, S. (1981) Mechanism of proteinase
507 complex formation with alpha 2-macroglobulin. Three modes of trypsin binding. *FEBS Lett*
508 **128**: 127–132.

509 Sottrup-Jensen, L., Sand, O., Kristensens, L., and Fey, G.H. (1989) The alpha-
510 macroglobulin bait region. *J Biol Chem* **264**: 15781–15789.

Stoops, J., Schroeter, J., Bretaudiere, J.-P., Olson, N., Baker, T., and Strickland, D. (1991) Structural studies of human alpha-2-macroglobulin : Concordance between projected views obtained by negative-stain and cryoelectron microscopy. *J Struct Biol* **106**: 172–178.

Varki, A., and Schauer, R. (2009) Sialic acids. In *Essentials of Glycobiology. 2nd edition.* Varki, A., Cummings, R., and Esko, J. (eds). Cold Spring Harbor (NY), Chapter 14.

Waddling, C., Plummer, T., Tarentino, A., and Roey, P. Van (2000) Structural basis for the substrate specificity of endo-beta-N-acetylglucosaminidase F(3). *Biochemistry* **39**: 7878–7885.

Walsh, C.T., Garneau-Tsodikova, S., and Gatto, G.J. (2005) Protein posttranslational modifications: the chemistry of proteome diversifications. *Angew Chem Int Ed Engl* **44**: 7342–7372.

Williams, S.E., Kounnas, M.Z., Argraves, K.M., Argraves, W.S., and Strickland, D.K. (1994) The alpha-2-macroglobulin receptor/low density lipoprotein receptor-related protein and the receptor-associated protein. An overview. *Ann N Y Acad Sci* **737**: 1–13.

Woessner, J.F. (1999) Matrix metalloproteinase inhibition from the Jurassic to the third millennium. *Ann New York Acad Sceinces* **878**: 388–403.

Table 1: Crystallization and X-ray diffraction of crystals.

Protein	Crystallization conditions	Crystal morphology	Diffraction resolution
Native hα_2M	0.2M lithium sulfate, 0.1M imidazole pH8.0 10% PEG 3000 At 20°C	Irregular crystals	-
Native hα_2M deglycosylated	-	Spherulites	-
Hα_2M-MA	0.1M Tris-HCl pH7.5 15% PEG 3350 At 20°C 0.2M ammonium citrate pH6.4 15% PEG 5000 MME At 20°C	Rectangular prisms Two dimensional plates	5.9Å
Hα_2M-MA deglycosylated	0.2M ammonium citrate pH6.4 15% PEG 5000 MME At 20°C	Rectangular prisms	7Å
Hα_2M deglycosylated in complex with thermolysin	0.1M MIB[1] pH8.0 25% PEG 1500 At 20°C	Rectangular prisms	8Å
Native ovostatin	0.2M NaCl 0.1M phosphate citrate pH5.0 10% PEG 3000 At 4°C	Square pyramids	10Å
Native ovostatin deglycosylated	-	Spherulites	-
Ovostatin in complex with chymotrypsin	0.1M MIB pH4.0 22% PEG 1500 At 4°C	Square pyramids	6.7Å
Ovostatin in complex with thermolysin	0.1M sodium acetate pH4.6 8% PEG 4000 At 4°C	Thin needles	-

[1]MIB buffer is produced by mixing sodium malonate, imidazole, and boric acid in the molar ratios 2:3:3.
Ha2M, human a2-macrogobulin.

547

548

Table 2: Crystallographic data.

Dataset	hα$_2$M-MA	Ovostatin in complex with chymotrypsin
Space group / cell constants (a, b, and c, in Å)	$P2_12_12_1$ / 130.1 262.7 281.5	$C222$ / 287.3 478.7 367.2
Wavelength (Å)	0.97917	0.97239
No. of measurements / unique reflections	160,377 / 25,026	615,133 / 45,268
Resolution range (Å) (outermost shell)[a]	49.23– 5.97 (6.66 – 5.97)	49.78 – 6.72 (7.34 – 6.72)
Completeness (%)	99.2 (99.7)	99.6 (100)
R_{merge}[b]	0.080 (0.628)	0.143 (0.801)
$R_{r.i.m.}$ (=R_{meas})[b]	0.087 (0.68)	0.148 (0.832)
Average intensity (<[<I> / σ(<I>)]>)	19.3 (3.2)	15.9 (4.08)
B-Factor (Wilson) (Å^2) / Average multiplicity	293.5/ 6.4 (6.6)	335.3/ 13.6 (13.8)

[a]Values in parentheses refer to the outermost resolution shell.
[b]$R_{r.i.m.} = \Sigma_{hkl}(n_{hkl} / [n_{hkl-1}]^{1/2})\Sigma_i |I_i(hkl) - \langle I(hkl)\rangle| / \Sigma_{hkl}\Sigma_i I_i(hkl)$ where $I_i(hkl)$ is the i-th intensity measurement and n_{hkl} the number of observations of reflection hkl,including symmetry-related reflections, and $\langle I(hkl)\rangle$ its average intensity. $R_{merge} = \Sigma_{hkl}\Sigma_i |I_i(hkl) - \langle I(hkl)\rangle| / \Sigma_{hkl}\Sigma_i I_i(hkl)$.

[Figure Legends]

Figure 1. Modification of native hα_2M and ovostatin by deglycosylation or activation to the induced form. **(A)** SDS-PAGE of hα_2M and ovostatin after isolation and purification from individual sources. **(B)(C)** Desialylation of ovostatin and hα_2M, respectively. Protein samples were incubated in the absence (*lane 1*) or presence (*lane 2*) of sialidase and analyzed by native PAGE. **(D)** Deglycosylation of hα_2M by PNGase F. Purified protein (*lane 1*) was digested with PNGase F (*lane 2*) in a weight ratio of 10:1 and analyzed by native PAGE. **(E)** Activation of hα_2M by methylamine. Deglycosylated hα_2M (*lane 1*) was induced with methylamine (*lane 2*) and analyzed by native PAGE. **(F)(G)** Deglycosylation of hα_2M and ovostatin by glycosidases. Protein samples were incubated in the absence (*lanes 1* and *7*) or presence of either PNGase F (*lane2*) or different Endo Fs (F1, F2 and F3) individually (*lanes 3-5*) or in a single reaction (lane 6) and subsequently analyzed by SDS-PAGE or native PAGE, respectively. **(H)** Thermal shift curves of native hα_2M and ovostatin before (black lines) and after deglycosylation (gray lines). Values are represented as means of three experiments. **(I)(J)** Activation of hα_2M and ovostatin by peptidases. Proteins were incubated with thermolysin or chymotrypsin at various ratios and analyzed by SDS-PAGE. The residual proteolytic activity (in box) against BODIPY FL-casein is expressed as percentage of the activity in absence of α_2M. Reactions were kept 30min at room temperature before fluorescence measurements.

Figure 2. Protein crystals of native and induced hα_2M and ovostatin. **(A)** Irregularly-shaped crystals of native hα_2M. **(B)** Spherulites formed in crystallization drops with deglycosylated native hα_2M. **(C)(D)** Prism-shaped crystals and two dimensional plates of methylamine induced hα_2M. **(E)(F)** Prism-shaped crystals of deglycosylated hα_2M in complex with thermolysin. **(G)** Pyramid-shaped crystals of native ovostatin. **(H)** Needle-shaped crystals of ovostatin in complex with thermolysin. **(I)** Pyramid-shaped crystals of ovostatin in complex with chymotrypsin.

Figure 3. Images of the diffraction pattern of **(A)** hα_2M and **(B)** ovostatin crystals after exposure to synchrotron radiation. Both images were obtained after 1^{o} rotation and

exposure for 0.5sec or 20sec at 100% transmission in ID23-1 or ID29, respectively. Black circles indicate the diffraction resolution.

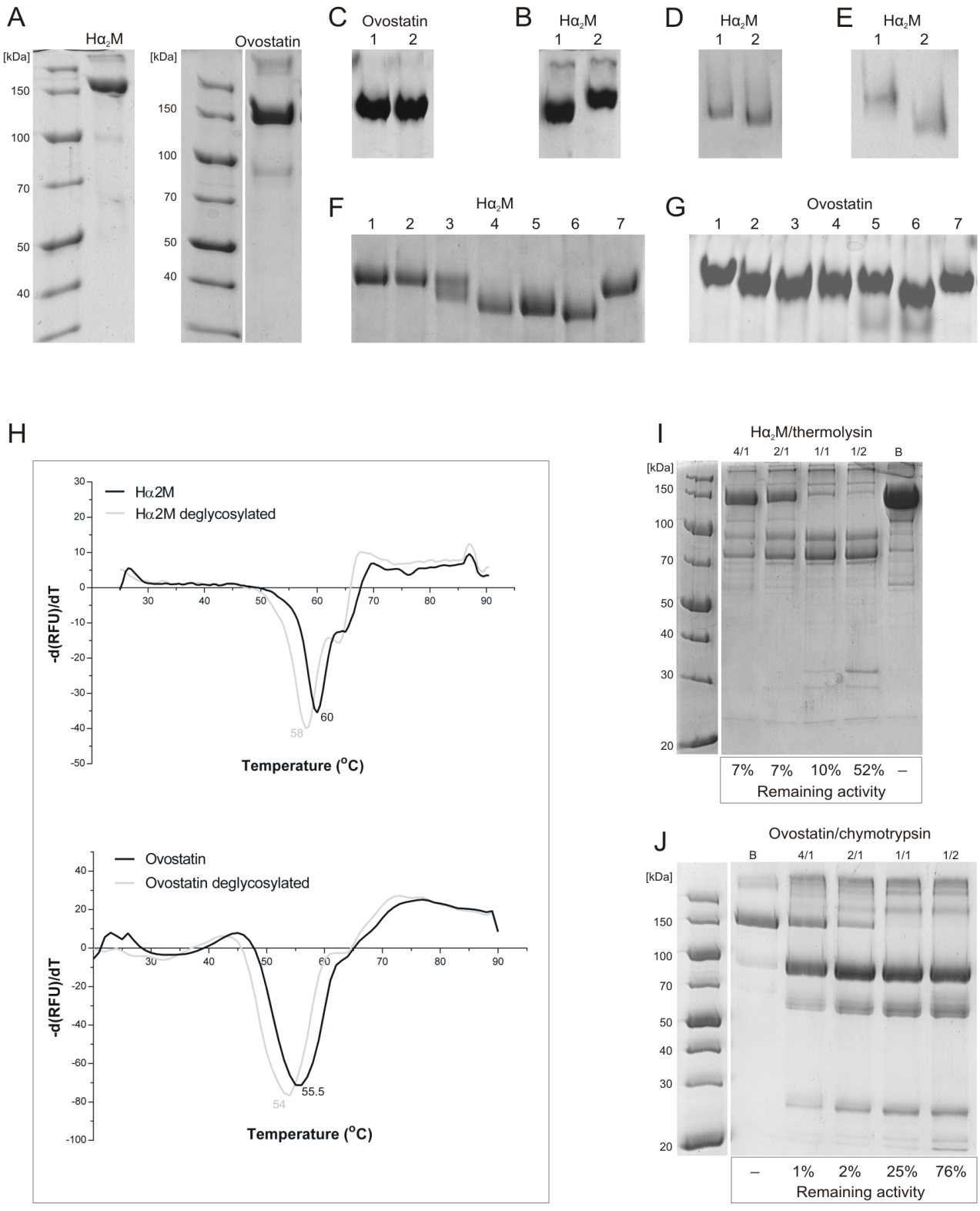
A
Hα2M
[kDa]
150
100
70
50
40
Ovostatin
[kDa]
150
100
70
50
40
C
Ovostatin
1 2
B
Hα2M
1 2
D
Hα2M
1 2
E
Hα2M
1 2
F
Hα2M
1 2 3 4 5 6 7
G
Ovostatin
1 2 3 4 5 6 7
H
Hα2M
Hα2M deglycosylated
-d(RFU)/dT
30 20 10 0 -10 -20 -30 -40 -50
30 40 50 60 70 80 90
60
58
Temperature (°C)
Ovostatin
Ovostatin deglycosylated
-d(RFU)/dT
40 20 0 -20 -40 -60 -80 -100
30 40 50 60 70 80 90
55.5
54
Temperature (°C)
I
Hα2M/thermolysin
4/1 2/1 1/1 1/2 B
[kDa]
150
100
70
50
40
30
20
7% 7% 10% 52% –
Remaining activity
J
Ovostatin/chymotrypsin
B 4/1 2/1 1/1 1/2
[kDa]
150
100
70
50
40
30
20
– 1% 2% 25% 76%
Remaining activity

A

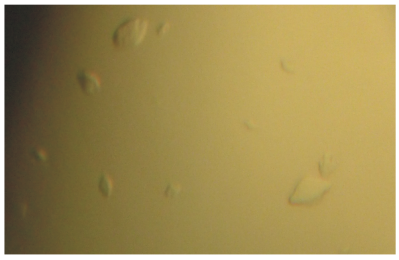

B

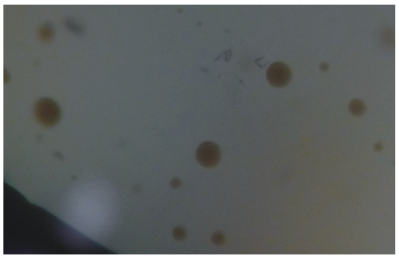

C

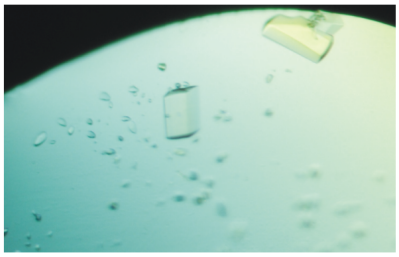

D

E

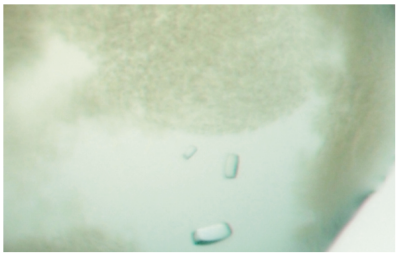

F

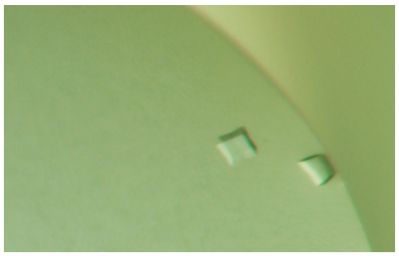

G

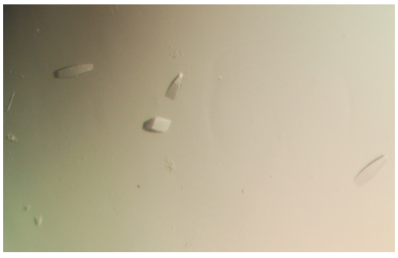

H

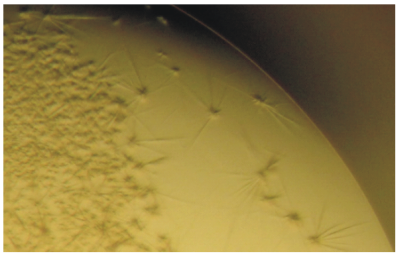

I

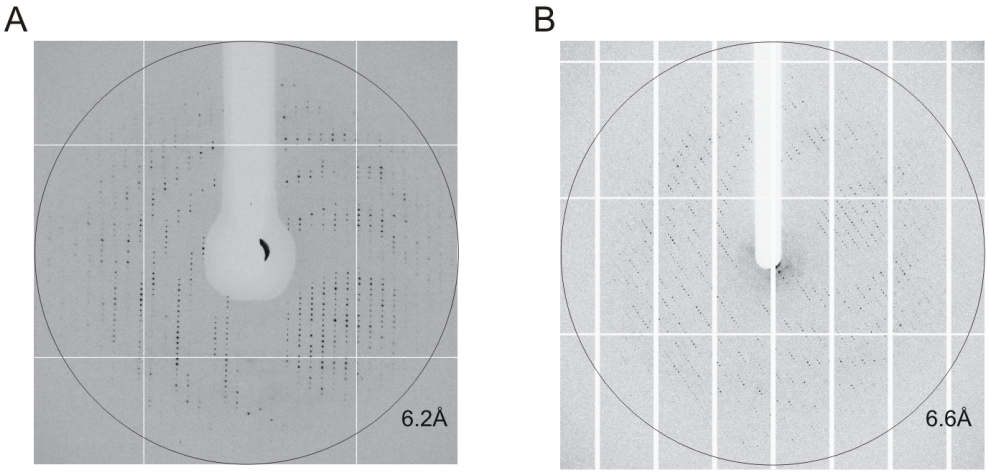
A
6.2Å
B
6.6Å